APPLIED AND ENVIRONMENTAL MICROBIOLOGY, May 1994, p. 1663–1669
0099-2240/94/$04.00+0
Copyright © 1994, American Society for Microbiology
Vol. 60, No. 5

Evaluation of Fleroxacin Activity against Established *Pseudomonas fluorescens* Biofilms

D. R. KORBER,[1,2]* G. A. JAMES,[1,3] AND J. W. COSTERTON[2]

Department of Biological Sciences, University of Calgary, Calgary, Alberta T2N 1N4,[3] and Department of Applied Microbiology and Food Science, University of Saskatchewan, Saskatoon, Saskatchewan S7N 0W0,[1] Canada, and Center for Biofilm Engineering, Montana State University, Bozeman, Montana 59717[2]

Received 28 September 1993/Accepted 9 February 1994

Scanning confocal laser microscopy (SCLM) and fluorescent molecular probes were used to evaluate the effect of the fluoroquinolone fleroxacin on the architecture of established *Pseudomonas fluorescens* biofilms. Control *P. fluorescens* biofilms were heterogeneous, consisting of cell aggregates extending from the attachment surface to maximum measured depths of ~90 μm (mean biofilm depth at 72 h, 42 ± 28 μm) and penetrated by an array of channels. In contrast, fleroxacin-treated biofilms were less deep (mean biofilm depth at 72 h, 29 ± 8 μm), varied little in depth over large areas, and consisted of a homogeneous distribution of cells. Fleroxacin also caused cells to elongate, with cells located near the biofilm-liquid interface lengthening significantly more than cells located at the attachment surface. By using SCLM, acridine orange, and image analysis it was found that ~59% of cells within fleroxacin-treated biofilms emitted red fluorescence whereas >99% of cells from control biofilms emitted green fluorescence. The fleroxacin-treated cells which emitted red fluorescence were observed to be the population of cells which elongated.

The efficacy of antimicrobial agents against surface-associated bacteria has been the subject of much medical and industrial concern. Attempts to evaluate the effectiveness of target compounds have primarily consisted of viable-cell-culture methodology (kill curves) (1, 25, 27, 32); however, visual indicators have potential for evaluating antibiotic effectiveness in microbial samples. A number of compounds (vital redox dyes and fluorogenic substrates) have been used to estimate bacterial metabolic potential in environmental samples. Cyanoditolyl tetrazolium chloride, 2-(*p*-iodophenyl)-3-(*p*-nitrophenyl)-5-phenyl tetrazolium chloride, nalidixic acid, fluorescein diacetate, and resazurin have all found applications during studies of cell metabolic activity (2–4, 8, 26, 29, 31, 35). Acridine orange (AO) is a commonly utilized fluorescent compound which specifically interacts with DNA and RNA by intercalation or electrostatic interactions and, on the basis of the configuration and concentration of the nucleic acids, strongly emits fluorescence in either the green or the red spectrum (emission maxima, 526 and 650 nm). The color of AO fluorescence has been used to estimate cellular viability, as distinctive RNA/DNA ratios and fluor-nucleotide configurations result from different growth or study conditions (13). However, inconsistencies in published results exist, with both viable and nonviable control cells reportedly emitting red fluorescence following AO treatment (2, 13, 19). Overall, few fluorescent indicators have been applied to in situ analysis of mature biofilms; therefore, there remains a need for these procedures to be refined or adapted for biofilm control applications.

Quinolone compounds target the A subunit of DNA gyrase, an enzyme responsible for supercoiling bacterial chromosomal DNA (9, 10). Bacteria which have incorporated these compounds are unable to supercoil their DNA, and therefore the nucleic acids in quinolone-treated cells are loosely coiled and significantly different from those in untreated cells. Molecular probes sensitive to nucleic acid configuration (e.g., AO) have potential for detecting the activity of gyrase-specific inhibitors. The present study involved exposing established *Pseudomonas fluorescens* biofilms to fleroxacin, thereby inhibiting the normal replication of DNA within biofilm bacteria susceptible to the compound. The effect of fleroxacin was then evaluated with respect to biofilm architecture and cellular morphology. The mechanism of quinolone activity also allowed the use of AO as a specific indicator of fleroxacin-affected bacteria.

P. fluorescens CC-840406-E was cultured in 0.3% (wt/vol) Trypticase soy broth (Difco Laboratories, Detroit, Mich.). Biofilm studies were initiated by inoculating 10-channel flow cells with log-phase cells obtained from 50-ml batch cultures grown in flasks on a gyratory shaker at 23 ± 2°C (22). Flow cells with internal channel dimensions of 1 by 3 by 45 mm were milled from a single piece of Lexan plastic; sterilization and inoculation of the flow cells were performed as previously described (23). After inoculation, flow cells were continuously irrigated with 0.3% Trypticase soy broth at a laminar flow velocity of 0.05 cm s^{-1} for 72 h with a Watson-Marlow 201Z multichannel peristaltic pump. Inoculated chambers were then mounted on the stage of a photomicroscope for analysis by scanning confocal laser microscopy (SCLM) while a continuous nutrient flow was maintained.

Fleroxacin (Ro 23-6240; AM 833) was obtained from Hoffmann-La Roche, Inc. (Nutley, N.J.), and added to the medium reservoir (final concentration, 2 μg ml^{-1}) following 24 h of biofilm growth. Biofilms were then incubated with a 0.05-cm s^{-1} flow rate in the presence of fleroxacin for an additional 24 and 48 h and compared with the fleroxacin-free control biofilms grown for the same periods. Short-term effects of fleroxacin on 24-h *P. fluorescens* biofilms were evaluated by pulse-injecting fleroxacin into the flow cells at concentrations of 1, 2, and 4,000 μg ml^{-1} for 90 min in the absence of flow. Flow was then reestablished at the previous rate to wash excess fleroxacin from the flow cell prior to epifluorescence microscopy examination to confirm the penetration of the fluorescent antibiotic (excitation maximum, 282 nm; emission maximum,

* Corresponding author. Mailing address: Applied Microbiology and Food Science, University of Saskatchewan, Saskatoon, Saskatchewan, Canada S7N 0W0. Phone: (306) 966-7704. Fax: (306) 966-8898.

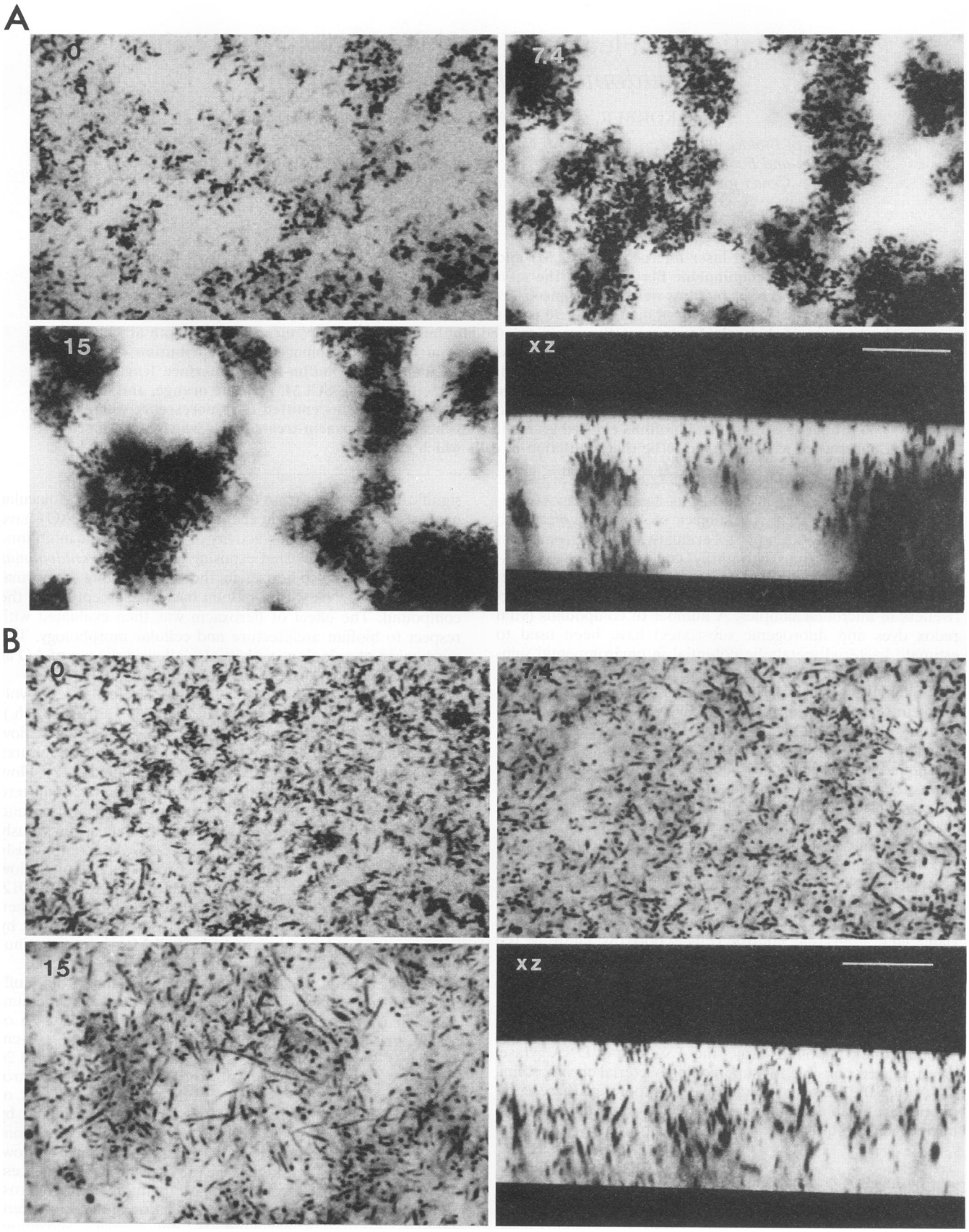
A
0
7.4
15
xz
B
0
7.4
15
xz

FIG. 1. Representative horizontal optical thin sections (0-, 7.4-, and 15-μm sampling depths, where 0 μm represents the attachment surface and 7.4 and 15 μm are distances from the attachment surface) obtained from control (A) and fleroxacin-treated (B) *P. fluorescens* biofilms after 48 h of biofilm development at a bulk flow rate of 10 ml h^{-1}. A 0.1% fluorescein solution was used to negatively stain the biofilms and allow imaging by SCLM. The lower right quadrant of the plate shows the biofilm in sagittal profile (*xz* optical thin section). In panel B, note the occurrence of elongated cells at the 7.4- and 15-μm sampling depths. Bar = 25 μm.

442 nm) into the biofilm bacteria. A solution of AO (0.1% [wt/vol]; Sigma, St. Louis, Mo.) was then injected into the flow cell for 2 min for use as a dual-wavelength-emission fluorescent probe specific for cellular nucleic acids. Excess AO was then washed from the flow cell by resuming flow before SCLM analysis. A negative stain was prepared as a 0.1% (wt/vol) fluorescein solution (molecular weight, 289; Sigma) and was aseptically added to the nutrient medium for SCLM examination of biofilm architecture and bacterial morphology (6, 7, 20).

Optical thin sections were obtained with an MRC-600 Lasersharp fluorescence scanning confocal laser system (Bio-Rad Microscience, Mississauga, Ontario, Canada) mounted on a Nikon FXA microscope equipped with a 60×, 1.4 numerical aperture objective (7, 21). An argon laser operated at 50 mW and 1% beam transmission was used as the excitation source for the fluorescein and AO fluorescent molecular probes. Simultaneous dual-channel imaging of green and red fluorescence from AO-treated samples involved the use of dual photodetectors and filter sets (540 DF 30 nm and EF 600 LP nm, respectively), whereas fluorescein imaging utilized fluorescence detection in the green spectrum (515 LP nm). Dual-channel and single-channel *xy* (horizontal optical thin section) and *xz* (vertical optical thin section) imaging was performed as previously reported (21, 25, 33).

The laser microscope system was integrated with a motorized, computer-controlled focusing system for vertical positioning during laser sectioning of biofilms, as well as a programmable *xy* stage system which defined the horizontal positioning. Optical thin sections from five depths within the biofilm (0, 3.7, 7.4, 11.1, and 15.0 μm from the attachment surface) were obtained from replicate locations for image analysis purposes. During the image acquisition process, the mean depths of the treatment and control biofilms were determined at random locations (n = 80). Control and fleroxacin-treated biofilms were then analyzed at different depths for cell biomass, cell aggregation, cell morphology, and wavelength of fluorescence emission (i.e., red or green fluorescence) by using either the image analysis software provided by Bio-Rad or an IBAS-2000 image processing computer (Kontron, Eching, Germany) (22). The aggregation index (AI) parameter was determined by dividing the total area of bacterial biomass measured for each sampling depth by the total number of bacterial aggregates. Aggregates were identified and enumerated by using computer image analysis at a constant thresholding level (7). Thus, high AI values correlated with the presence of aggregated cells. Photographs of optical thin sections were obtained by directly photographing digital images on the computer color monitor. Statistical analyses were performed with SYSTAT statistical software (Systat Inc., Evanston, Ill.) for the MacIntosh computer.

Architectural analysis of control *P. fluorescens* biofilms. It has been demonstrated that both pure culture and native biofilms grown for extended periods under flowing conditions frequently develop pores and channels (19, 21, 24, 34). Control *P. fluorescens* biofilms used during this study further confirmed these reports. Observed by SCLM at 24, 48, and 72 h, the control biofilms were found to consist of an extensive network of cell aggregates separated by water channels occurring at 20- to 40-μm intervals (Fig. 1A). This arrangement of cells and channels likely facilitated the diffusion of nutrients, oxygen, and wastes into and out of the biofilm matrix (11, 21, 24, 25). Image analysis of 48-h control biofilms revealed that the distribution of cellular biomass (in square micrometers) was lowest at the base, becoming increasingly dense further from the attachment surface and ranging from 301 ± 71 μm^2 at the 0-μm sampling depth to 886 ± 180 μm^2 at the 15-μm sampling depth (Fig. 2). This trend agreed with the tendency of the biofilm cells to form dense aggregates at regions further from the base of the biofilm (correlation coefficient = 0.959; r^2 = 0.919), as determined by using the AI parameter (Fig. 2). The presence of diffuse basal regions has previously been observed in biofilms during comparative studies between motile and nonmotile strains of *P. fluorescens*, in which biofilms formed by motile *P. fluorescens* were observed to develop zones near the base of the biofilm which possessed less cell material than was present in overlying cell layers (21, 24). Potential advantages of maintaining a minimal basal layer of cells within microbial films have previously been suggested (21, 25), and they include the enhanced diffusion of essential nutrients to these regions, as well as the removal of inhibitory waste products.

The control biofilms increased in depth from a mean value of 32 ± 14 μm at 48 h to 42 ± 28 μm after 72 h of biofilm development. The large standard deviation relative to the

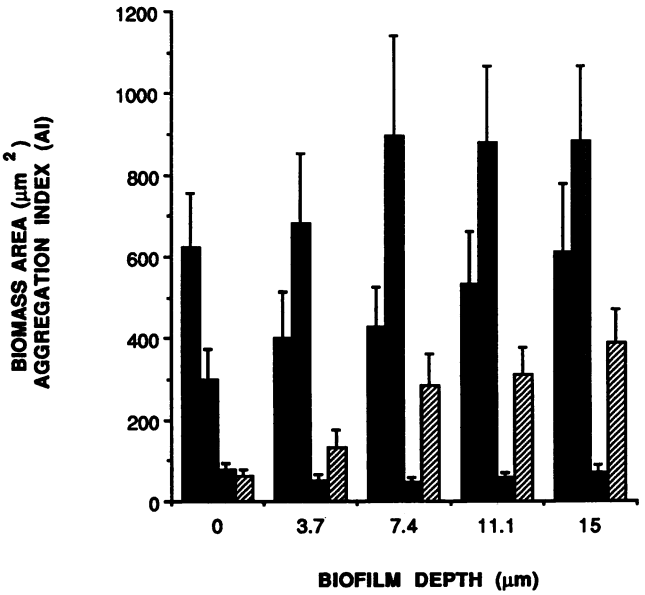

FIG. 2. Biomass area and AI determinations for the 0-, 3.7-, 7.4-, 11.1-, and 15-μm sampling depths of negatively stained control and fleroxacin-treated *P. fluorescens* biofilms at 48 h. Biomass area and aggregation measurements were determined by image analysis and reflect the area of all cell material detected and the horizontal-plane cell aggregation tendencies, respectively. Symbols: ▨ and ■, biomass area for control and fleroxacin-treated biofilms, respectively; ▨ and ▩, AI for control and fleroxacin-treated biofilms, respectively.

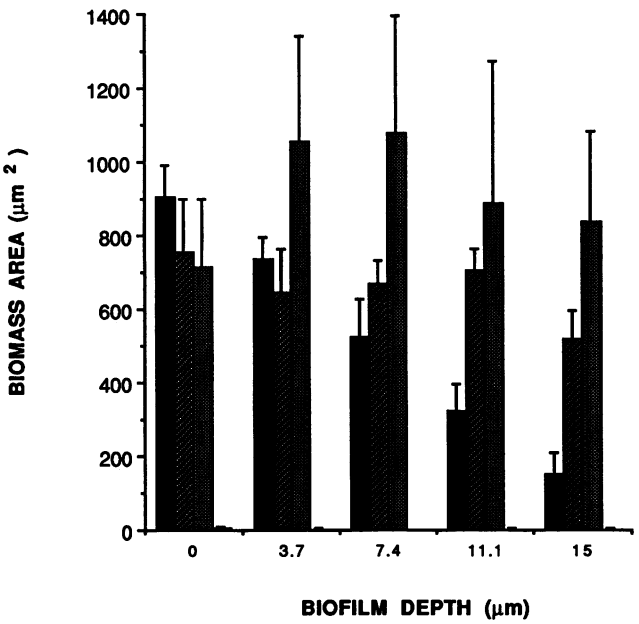

FIG. 3. Biomass area of red- and green-fluorescence-emitting material within AO-stained control and fleroxacin-treated *P. fluorescens* biofilms at 48 h. Biomass determinations were made by analyzing the 0-, 3.7-, 7.4-, 11.1-, and 15-μm sampling depths by image analysis. Symbols: ■ and ▨, green and red emissions from fleroxacin-treated biofilms, respectively; ▩ and ▨, green and red emissions from control biofilms, respectively.

mean biofilm depth reflected the presence of channels which penetrated to the base of the biofilm and thus had a measured height of ~0 μm. In absolute terms, control biofilms ranged in depth from 0 to 70 μm at 48 h and from 0 to 95 μm at 72 h. Similar observations have resulted from the study of steady-state *Pseudomonas aeruginosa* biofilms, in which a mean biofilm depth of 33 μm was measured but depths ranged from 13.3 to 60.0 μm (34). As channels were consistently observed in *P. fluorescens* biofilms following 24, 48, and 72 h of slide culture, recurring patterns present in biofilms likely represent an evolutionarily defined response by aerobic *P. fluorescens* biofilm-forming bacteria to oxygen- or nutrient-limiting growth conditions encountered within the film.

Architectural analysis of fleroxacin-treated *P. fluorescens* biofilms. Treated biofilms were not exposed to fleroxacin until 24 h and thus were identical to the control biofilms in all respects prior to addition of the fluoroquinolone. The concentration of fleroxacin used during biofilm studies was 12.5 times greater than the MIC determined for suspended-phase *P. fluorescens* (0.16 μg ml^{-1}; data not shown), in accordance with the relatively high level of resistance of biofilm bacteria to antibiotics and antimicrobial agents (12, 15, 28). Following the application of 2 μg of fleroxacin ml^{-1}, the biofilms underwent an architectural change. Within the 24 h following application of fleroxacin, channels and cell aggregates normally observed throughout the *P. fluorescens* biofilms were no longer evident and had been replaced by an even distribution of cells at all sampling depths (Fig. 1B). At the attachment surface, cell material was present at 622 ± 134 μm^2 per field of analysis, whereas 15 μm from the attachment surface 610 ± 170 μm^2 of cell material was detected (Fig. 2). No significant differences ($P \leq 0.05$) between cellular biomass measurements at the different depths (0, 3.7, 7.4, 11.1, and 15 μm) within the fleroxacin-treated biofilms were found. However, cell biomass measurements from all depths of the fleroxacin-treated biofilms were significantly different from measurements at the corresponding depths of the control biofilms ($P \leq 0.05$).

While the fleroxacin-treated biofilms did possess more biofilm material at the attachment surface than the control biofilms, this trend was reversed at all other biofilm depths. Consequently, the total biomass area from all sampling depths was greater for the control biofilms than for fleroxacin-treated biofilms (3,647 versus 2,599 μm^2, respectively). Furthermore, the AI was in agreement with other indications that the fleroxacin-treated biofilms consisted of more evenly distributed cells, with control AI values exceeding those determined for the fleroxacin biofilms by a factor of ~2 at the attachment surface and by a factor of >3.5 at a distance of 15 μm from the attachment surface (Fig. 2). There was no statistically significant correlation between the tendency of cells within fleroxacin-treated biofilms to aggregate and sampling depth (correlation coefficient = −0.604; $r^2 = 0.365$).

The bacteriostatic effect of fleroxacin was evidenced by that fact that the vertical development of fleroxacin-treated biofilms was significantly less ($P \leq 0.05$) than the control biofilms. At 48 h (24 h of exposure to fleroxacin), the mean biofilm depth was 23 ± 5 μm, whereas after 48 h of exposure to fleroxacin, the mean biofilm depth had increased only approximately 6.5 μm, to 29 ± 8 μm. This increase in biofilm depth was likely the result of the elongation of fleroxacin-affected cells. The small standard deviation of biofilm depth data for the fleroxacin-treated biofilms reflected the even, consistent nature of these systems. Channels were not present in fleroxacin-treated biofilms, with the structures apparently having filled in following the initial fleroxacin application. Figure 1B (*xz* sagittal section) shows the even distribution of cells within fleroxacin-treated biofilms as well as the absence of channels.

Effect of fleroxacin treatment on cell morphology. Fleroxacin treatment caused a gradient of cell elongation within the biofilm, with the greatest amount of cell elongation occurring near the biofilm-liquid interface. Bacteria positioned at the base of biofilms were not seen to elongate following 1.5 h, and they elongated only slightly after 24 h of exposure to 2 μg of fleroxacin ml^{-1} (total elapsed time, 48 h), whereas after 48 h of exposure all cells increased in length. At 48 h the control biofilm cells were 1.5 ± 0.5 μm in length, whereas fleroxacin-treated cells were 2.0 ± 0.7 μm in length. The length of control cells located at the base of the biofilm changed little after 72 h growth; however, the length of fleroxacin-treated cells increased to 4.2 ± 1.8 μm. While cell elongation occurred throughout fleroxacin-treated biofilms after 72 h, the greatest effect was observed at the 15-μm sampling depth, resulting in mean cell lengths of 8.1 ± 2.4 μm (maximum, >12 μm). In contrast, the control biofilm cells at the 15-μm sampling depth were 1.7 ± 0.6 μm long. Nalidixic acid has previously been used to estimate cell growth potential on the basis of the amount of cell elongation occurring following exposure to the gyrase-inhibiting compound (4). The analogous mode of action of fleroxacin should thus allow the comparison of relative growth potential of cells within biofilms. The gradient of cell elongation observed within fleroxacin-treated biofilms suggests that cells nearest the biofilm-liquid interface were growing more rapidly than cells deeply embedded within the biofilm matrix. Slow growth has previously been implicated in antibiotic resistance (5, 16, 17); therefore, a gradient of growth rates in naturally occurring biofilms provides an explanation for the

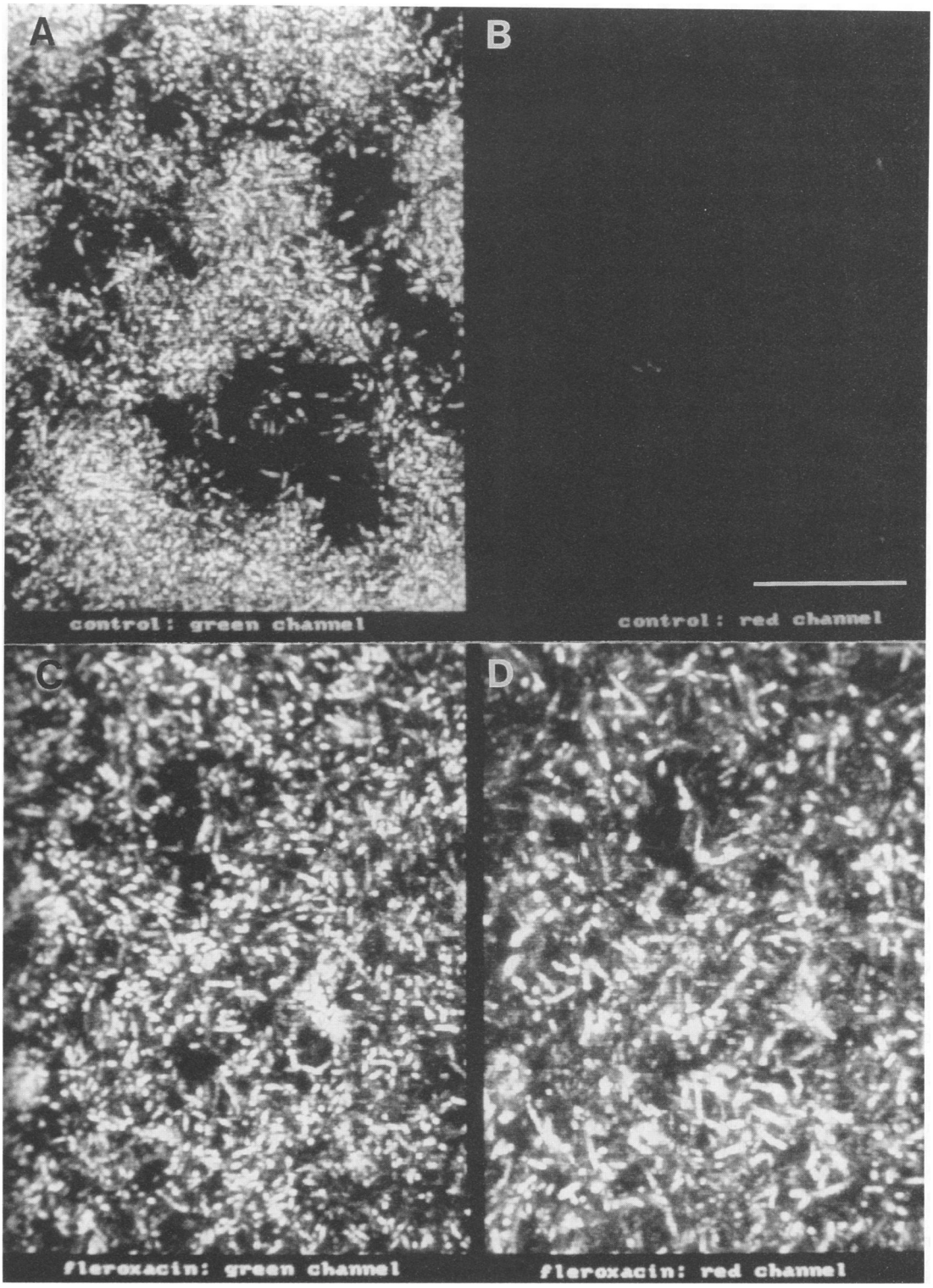

FIG. 4. Dual-channel optical thin sections showing the differential fluorescence emissions resulting from AO staining of 48-h control and fleroxacin-treated *P. fluorescens* biofilms. The AO-stained control biofilm primarily emitted green fluorescence (A), whereas the fleroxacin-treated biofilm contained large numbers of cells which fluoresced red (D). Bar = 50 μm.

persistence of surface-associated bacteria subjected to traditional control strategies.

In addition to inducing cell elongation, fleroxacin also caused some cells to undergo a gross morphological change, resulting in massive, rounded cells apparently unable to divide but capable of significant growth. These pleomorphic cells were mainly oval and were observed singly and not in groups. Elongated and rounded cells were not detected at any depth or

at any stage of control biofilm development during these studies.

Examination of cell metabolic state by using SCLM and AO. AO was used to estimate the number of fleroxacin-affected cells within the biofilm. The percentage of red cells varied with the distance from the attachment surface within the fleroxacin-treated biofilms. At 48 h, ~45% of the cells present emitted red fluorescence at the 0-μm sampling depth; these values increased significantly ($P \leq 0.05$) to the maximum measured percentage of red cells at the 15-μm sampling depth (~77% of all measured cells fluoresced red) (Fig. 3). In contrast, cells within the control biofilms were consistent with depth, with >99% of the cells at the 0-, 3.7-, 7.4-, 11.1-, and 15-μm sampling depths emitting green fluorescence (Fig. 3). Overall, the zones where fleroxacin-induced cell elongation was most prevalent were the regions where the greatest percentage of red fluorescence-emitting cells were detected (Fig. 3 and 4). Earlier studies have shown that when the permeability of the cell outer membrane was increased by using Triton X-100, an increase in the number of orange or red AO-stained cells from 5 to 60% was observed (30). Thus, fleroxacin, which has a similar outer membrane-permeabilizing effect (36), may have contributed to the occurrence of red fluorescence in elongated cells.

The utility of AO as a viability indicator or, in this case, as an indicator of fleroxacin effectiveness is based on the proportion of single-stranded nucleic acids to double-stranded nucleic acids within the cell (13). High RNA/DNA ratios have been correlated with rapid cell growth, whereas low ratios have been associated with dead or slowly growing cells (14). Once AO binds nucleic acids, the resultant fluor-nucleotide configuration (i.e., whether the probe is bound to a monomerically to double-stranded DNA or dimerically to single-stranded RNA or denatured DNA) affects the wavelength of fluorescence emission from the cell, thereby providing an indication of the cell metabolic state. However, published results dealing with this topic vary. Keevil and Walker (19) observed that slowly growing cells having tightly coiled DNA and a low RNA content fluoresced green following intercalation of AO with nucleic acid. In a review by Daley (13), it was stated that AO used in combination with single-stranded nucleic acids resulted in red fluorescence whereas green fluorescence was observed when AO was used in combination with double-stranded nucleic acids. Others have reported that the color of fluorescence emission varied depending on the concentrations of AO, heat treatments, or the presence of membrane-permeabilizing agents (2, 13, 18, 19). During the present study, DNA gyrase inhibition would similarly result in loosely coiled DNA and, in conjunction with outer membrane-permeabilizing effects, would account for the staining specificity (red fluorescence) of AO during these studies and allow the identification of biofilm bacteria affected by fleroxacin.

Conclusions. The architecture normally evident within established *P. fluorescens* biofilms was altered by the addition of the quinolone compound fleroxacin. Following a minimum of 24 h of fleroxacin exposure, biomass measurements at various depths, biofilm thickness, and cellular morphology all varied from the control biofilm results. Channels prevalent within *P. fluorescens* biofilms were disrupted by fleroxacin treatment. Furthermore, there was a gradient effect of fleroxacin action among biofilm bacteria, with cells nearest the biofilm-liquid interface undergoing greater elongation than cells near the attachment surface. The elongated-cell population correlated with cells which emitted red fluorescence following AO treatment. The results of this study indicate that molecular and morphological indicators of cell metabolism may find applications in biofilm studies of antimicrobial effects. In this case, AO provided a mechanism for identifying fleroxacin-affected cells, the specificity of which was confirmed by using a secondary visual indicator, the occurrence of elongated cells unable to divide.

We thank D. E. Caldwell for the use of the Laser Microscopy/Digital Imaging facility at the University of Saskatchewan. Also acknowledged are Hoffmann-La Roche and Barbara Prosser for providing fleroxacin for use in this study.

REFERENCES

1. **Anwar, H., and J. W. Costerton.** 1990. Enhanced activity of combinations of tobramycin and piperacillin for eradication of sessile biofilm cells of *Pseudomonas aeruginosa*. Antimicrob. Agents Chemother. **34**:1666–1671.
2. **Back, J. P., and R. G. Kroll.** 1991. The differential fluorescence of bacteria stained with acridine orange and the effects of heat. J. Appl. Bacteriol. **71**:51–58.
3. **Betts, R. P., P. Bankes, and J. G. Banks.** 1989. Rapid enumerations of viable micro-organisms by staining and direct microscopy. Lett. Appl. Microbiol. **9**:199–202.
4. **Bottomley, P. J., and S. P. Maggard.** 1990. Determination of viability within serotypes of a soil population of *Rhizobium leguminosarum* bv. *trifolii*. Appl. Environ. Microbiol. **56**:533–540.
5. **Brown, M. R. W., D. G. Allison, and G. Gilbert.** 1988. Resistance of bacterial biofilms to antibiotics: a growth-rate related effect? J. Antimicrob. Chemother. **22**:777–780.
6. **Caldwell, D. E., D. R. Korber, and J. R. Lawrence.** 1992. Imaging of bacterial cells by fluorescence exclusion using scanning confocal laser microscopy. J. Microbiol. Methods **15**:249–261.
7. **Caldwell, D. E., D. R. Korber, and J. R. Lawrence.** 1992. Confocal laser microscopy and computer image analysis. Adv. Microb. Ecol. **12**:1–67.
8. **Caldwell, D. E., and J. R. Lawrence.** 1989. Microbial growth and behavior within surface microenvironments, p. 140–145. *In* T. Hattori, Y. Ishida, Y. Maruyama, R. Y. Morita, and A. Uchida (ed.), Proceedings of ISME-5. JSS Press, Tokyo.
9. **Chapman, J. S., and N. H. Georgopapadakou.** 1988. Routes of quinolone permeation in *Escherichia coli*. Antimicrob. Agents Chemother. **32**:438–442.
10. **Chapman, J. S., and N. H. Georgopapadakou.** 1989. Fluorometric assay for fleroxacin uptake by bacterial cells. Antimicrob. Agents Chemother. **28**:581–586.
11. **Characklis, W. G., G. A. McFeters, and K. C. Marshall.** 1990. Physiological ecology in biofilm systems, p. 341–393. *In* W. G. Characklis and K. C. Marshall (ed.), Biofilms. J. Wiley & Sons, New York.
12. **Costerton, J. W., T. J. Marrie, and K.-J. Cheng.** 1985. Phenomena of bacterial adhesion, p. 3–43. *In* D. C. Savage and M. Fletcher (ed.), Bacterial adhesion: mechanisms and physiological significance, Plenum Press, New York.
13. **Daley, R. J.** 1979. Direct epifluorescence enumeration of native aquatic bacteria: uses, limitations, and comparative accuracy. ASTM Spec. Tech. Publ. **695**:29–45.
14. **DeLong, E. F., G. S. Wickham, and N. R. Pace.** 1989. Phylogenetic stains: ribosomal RNA-based probes for the identification of single cells. Science **243**:1360–1363.
15. **Duguid, L. G., E. Evans, M. R. W. Browns, and P. Gilbert.** 1992. Growth-rate-independent killing by ciprofloxacin of biofilm-derived *Staphylococcus epidermidis*; evidence for cell-cycle dependency. J. Antimicrob. Chemother. **30**:791–802.
16. **Eng, R. H. K., F. T. Padberg, S. M. Smith, E. N. Tan, and C. E. Cherubin.** 1991. Bactericidal effects of antibiotics on slowly growing and nongrowing bacteria. Antimicrob. Agents Chemother. **35**:1824–1828.
17. **Gilbert, P., P. J. Collier, and M. R. W. Brown.** 1990. Influence of growth rate on susceptibility to antimicrobial agents: biofilms, cell cycle, dormancy, and stringent response. Antimicrob. Agents Chemother. **34**:1856–1868.
18. **Hobbie, J. E., R. J. Daley, and S. Jasper.** 1977. Use of Nuclepore filters for counting bacteria by fluorescence microscopy. Appl.

Environ. Microbiol. **33:**1225–1228.
19. **Keevil, C. W., and J. T. Walker.** 1992. Normarski DIC microscopy and image analysis of biofilms. Binary **4:**93–95.
20. **Korber, D. R., J. R. Lawrence, M. J. Hendry, and D. E. Caldwell.** 1992. Programs for determining representative areas of microbial biofilms. Binary **4:**204–210.
21. **Korber, D. R., J. R. Lawrence, M. J. Hendry, and D. E. Caldwell.** 1994. Analysis of spatial variability within mot$^+$ and mot$^-$ *Pseudomonas fluorescens* biofilms using representative elements. Biofouling **7:**339–358.
22. **Korber, D. R., J. R. Lawrence, B. Sutton, and D. E. Caldwell.** 1989. Effect of laminar flow velocity on the kinetics of surface recolonization by mot$^+$ and mot$^-$ *Pseudomonas fluorescens*. Microb. Ecol. **18:**1–19.
23. **Korber, D. R., J. R. Lawrence, L. Zhang, and D. E. Caldwell.** 1990. Effect of gravity on bacterial colonization in laminar flow environments. Biofouling **2:**335–350.
24. **Lawrence, J. R., and D. R. Korber.** 1993. Aspects of microbial surface colonization behavior, p. 113–118. *In* R. Guerrero and C. Pedrós-Alió (ed.), Trends in microbial ecology. Spanish Society for Microbiology, Barcelona.
25. **Lawrence, J. R., D. R. Korber, B. D. Hoyle, J. W. Costerton, and D. E. Caldwell.** 1991. Optical sectioning of microbial biofilms. J. Bacteriol. **173:**6558–6567.
26. **Marxsen, J.** 1988. Investigations into the number of respiring bacteria in groundwater from sandy and gravelly deposits. Microb. Ecol. **16:**65–72.
27. **Nichols, W. W., S. M. Dorrington, M. P. E. Slack, and H. L. Walmsley.** 1988. Inhibition of tobramycin diffusion by binding to alginate. Antimicrob. Agents Chemother. **32:**518–523.
28. **Nickel, K. C., I. Ruseska, and J. W. Costerton.** 1985. Tobramycin resistance of cells of *Pseudomonas aeruginosa* growing as a biofilm on urinary catheter material. Antimicrob. Agents Chemother. **27:**619–624.
29. **Nix, P. G., and M. M. Daykin.** 1992. Resazurin reduction tests as an estimate of coliform and heterotrophic bacterial numbers in environmental samples. Bull. Environ. Contam. Toxicol. **49:**354–360.
30. **Pettipher, G. L., and U. M. Rodrigues.** 1981. Rapid enumeration of bacteria in heat-treated milk and milk products using a membrane filtration-epifluorescent microscopy technique. J. Appl. Microbiol. **50:**157–166.
31. **Rodriguez, G. G., D. Phipps, K. Ishiguro, and H. F. Ridgway.** 1992. Use of a fluorescent redox probe for direct visualization of actively respiring bacteria. Appl. Environ. Microbiol. **58:**1801–1808.
32. **Ruseska, I., J. Robbins, J. W. Costerton, and E. S. Lashen.** 1982. Biocide testing against corrosion-causing oil-field bacteria helps control plugging. Oil Gas J. **80:**253–264.
33. **Shotton, D. M.** 1989. Confocal scanning optical microscopy and its applications for biological specimens. J. Cell Sci. **94:**175–206.
34. **Stewart, P. S., B. M. Peyton, W. J. Drury, and R. Murga.** 1993. Quantitative observations of heterogeneities in *Pseudomonas aeruginosa* biofilms. Appl. Environ. Microbiol. **59:**327–329.
35. **Tabor, P. S., and R. A. Neihof.** 1982. Improved method for determination of respiring individual microorganisms in natural waters. Appl. Environ. Microbiol. **43:**1249–1255.
36. **Vaara, M.** 1992. Agents that increase the permeability of the outer membrane. Microbiol. Rev. **65:**395–411.